

The Central Regions of Early-Type Galaxies Hosting Active Galactic Nuclei as viewed with *HST*/NICMOS

Swara Ravindranath^{1,2}, Luis C. Ho¹, C. Y. Peng³, A. V. Filippenko², and W. L. W. Sargent⁴

¹ The Observatories of the Carnegie Institution of Washington, 813 Santa Barbara Street, Pasadena, CA 91101

² Astronomy Department, University of California, Berkeley, CA 94720–3411

³ Steward Observatory, University of Arizona, Tucson, AZ 85721

⁴ Palomar Observatory, Caltech 105–24, Pasadena, CA 91125

Abstract. We present preliminary results from surface photometry of a sample of early-type galaxies observed with NICMOS on board *HST* in the F160W (*H*-band) filter. Dust is found to occur mostly in galaxies which possess unresolved nuclei, and in a few cases the presence of dust causes the isophotes to appear boxy. We performed a 2-D modeling of the host galaxy light distribution using the empirical Nuker function, which proves to be an adequate representation of the surface brightness profile for most early-type galaxies. The accurate modeling of the bulge light allows us to obtain the magnitude of the unresolved central source without contamination from the underlying stellar population. Our classification of early-type galaxies into core-type and power-law galaxies agrees with the results from previous work based on *HST* optical images, with core profiles occurring in luminous galaxies and power-law profiles occurring in low-luminosity galaxies with disk isophotes. We do not find a dichotomy in the distribution of inner slopes. Unresolved nuclear point sources are evident in about one-third of the sample galaxies, with magnitudes in the range $13.5 \leq m_H \leq 17.3$. Most of the type 1 Seyfert and LINER nuclei (83%) reveal a distinct point source, while the detection rate is much less for type 2 nuclei (35%). The occurrence of point sources appears to be independent of whether the underlying galaxy has core-type profile or power-law profile.

1. Introduction

Images of the central regions of galaxies at *HST* resolution have made it possible to probe structures very close to the nucleus and to reveal unresolved point sources or compact star clusters. Optical images obtained using *HST* showed that the King model and the de Vaucouleurs $r^{1/4}$ law which were conventionally used to describe the surface brightness profiles of early-type galaxies do not provide a good fit for the regions within $\sim 10''$ (Ferrarese et al. 1994; Lauer et al. 1995; Carollo et al. 1997; Faber et al. 1997). The surface brightness profiles in the central

regions can be parameterized by the empirical “Nuker” function, which is essentially a double power-law of the form

$$I(r) = 2^{(\beta-\gamma)/\alpha} I_b \left(\frac{r_b}{r}\right)^\gamma \left[1 + \left(\frac{r}{r_b}\right)^\alpha\right]^{(\gamma-\beta)/\alpha}, \quad (1)$$

where β is the slope outside the break radius r_b , γ is the inner slope, α controls the sharpness of the transition between the outer and inner slopes, and I_b is the surface brightness at the break radius (Lauer et al. 1995). Early-type galaxies can be classified into core-type or power-law systems based on their surface brightness profiles. Core-type galaxies show a significant change in the slope of the surface brightness profile within the break radius r_b with the inner slope γ being much shallower than for the outer regions. Power-law galaxies have profiles that show no significant change in slope within the inner $10''$ and remain as steep power laws all the way to the resolution limit ($r = 0.1''$). A value of $\gamma < 0.3$ is adopted as the criterion for classifying a galaxy as a core-type. Faber et al. (1997) found that no galaxies had γ in the range 0.3 to 0.5 and therefore that there was a clear dichotomy in the distribution of γ values between core galaxies and power-law galaxies. Interestingly, the surface brightness profiles derived from WFPC2 *V*-band images of early-type galaxies with kinematically distinct cores yielded values of γ between 0.3 and 0.5, thereby removing the dichotomy (Carollo et al. 1997). Surface photometry of early-type galaxies based on *H*-band images from *HST* have been presented by Quillen, Bower, & Stritzinger (2000), along with the analytic Nuker fits, but they did not decouple the contributions from the bulge and point sources.

In this work, we aim to model the galaxy surface brightness closely and to extract the point source magnitudes free from contamination by the bulge light, for a sample of galaxies that host AGNs. Parameterizing the bulge and nucleus as separate components enables us to probe the relationship between the properties of the host galaxy and the nuclear activity. The NIR images are most suitable for deriving the surface brightness profiles because

Table 1. Properties of sample galaxies^a

Galaxy	Hubble Type	B_T	M_B^o	Spectral Class
NGC 221	E2	9.0	-15.5	A
NGC 404	S0	11.2	-15.9	L2
NGC 474	S0	12.3	-20.5	L2 ::
NGC 524	S0	11.3	-21.3	T2 ::
NGC 821	E6?	11.6	-20.1	A
NGC 1052	E4	11.4	-19.9	L1.9
NGC 2685	SB0	12.1	-19.2	S2/T2
NGC 3115	S0	9.8	-19.3	A
NGC 3379	E1	10.2	-19.3	L2/T2 ::
NGC 3384	SB0	10.8	-18.7	A
NGC 3593	S0/a	11.8	-17.2	H
NGC 3900	S0	12.2	-20.1	L2 :
NGC 4026	S0	11.6	-19.5	A
NGC 4111	S0 spin	11.6	-19.5	L2
NGC 4143	SAB0	11.6	-19.2	L1.9
NGC 4150	S0	12.4	-17.5	T2
NGC 4261	E2	11.4	-21.3	L2
NGC 4278	E1	11.0	-18.9	L1.9
NGC 4291	E	12.4	-20.0	A
NGC 4374	E1	10.0	-21.1	L2
NGC 4406	E3	9.8	-21.3	A
NGC 4417	SB0 : spin	12.0	-19.1	A
NGC 4472	E2	9.3	-21.8	S2 ::
NGC 4589	E2	11.6	-20.7	L2
NGC 4636	E0	10.4	-20.7	L1.9
NGC 5273	S0	12.4	-19.2	S1.5
NGC 5548	S0/a	13.3	-21.3	S1.5
NGC 5838	S0	11.9	-20.5	T2 ::
NGC 5982	E3	12.0	-20.8	L2 ::
NGC 6340	S0/a	11.8	-20.0	L2
NGC 7457	S0	12.0	-18.6	A
NGC 7626	E : pec	12.1	-21.2	L2 ::
NGC 7743	SB0	12.3	-19.7	S2

^a Galaxy properties taken from Ho et al. (1997)

of the reduced contamination from dust and young star clusters, and they sample the underlying smooth stellar population better than optical images.

2. The Sample and Data Analysis

Early-type (E and S0) galaxies were selected from the sample of galaxies (Table 1) studied spectroscopically by Ho, Filippenko, & Sargent (1997). Archival *HST* NICMOS images are available for 33 of these galaxies (14 E, 16 S0, and 3 S0/a) from different snapshot survey programs. The data were obtained in the F160W filter using NIC2 and NIC3 cameras. The NIC2 images have a field of view of $19''.2 \times 19''.2$ with a scale of $0''.076/\text{pixel}$. The NIC3 images have a field of view of $51''.2 \times 51''.2$ with a scale of $0''.2/\text{pixel}$. The CalnicA images were used after performing additional steps suggested in the NICMOS handbook which include pedestal removal, creating bad pixel masks, and interpo-

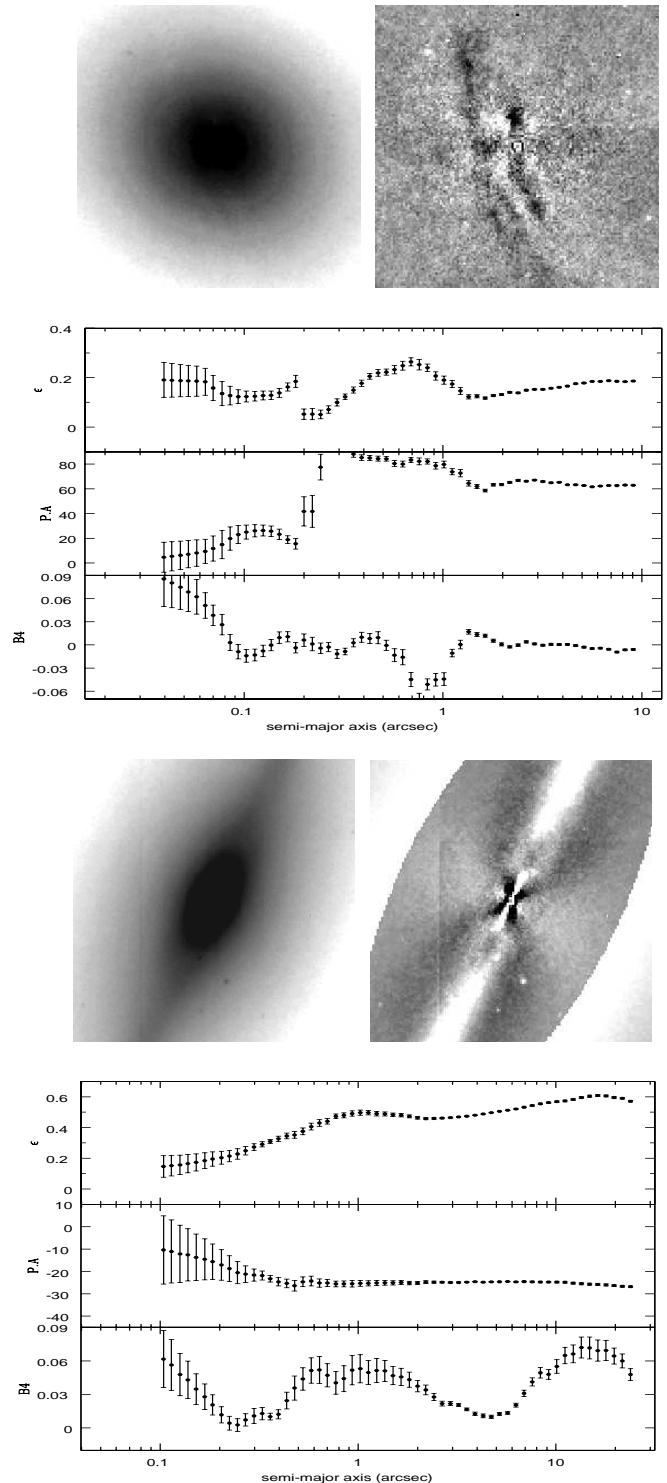


Fig. 1. The results of isophotal analysis are shown for NGC 4374 (*top*) and NGC 3115 (*bottom*). The left image is the observed *H*-band image and the right image is the residual after subtracting the model derived from elliptical isophotes. Each image is $10'' \times 10''$ and is centered on the galaxy. The orientation is arbitrary. The lower panels show the variation of ellipticity, position angle, and the shape parameter (B_4) along the semi-major axis.

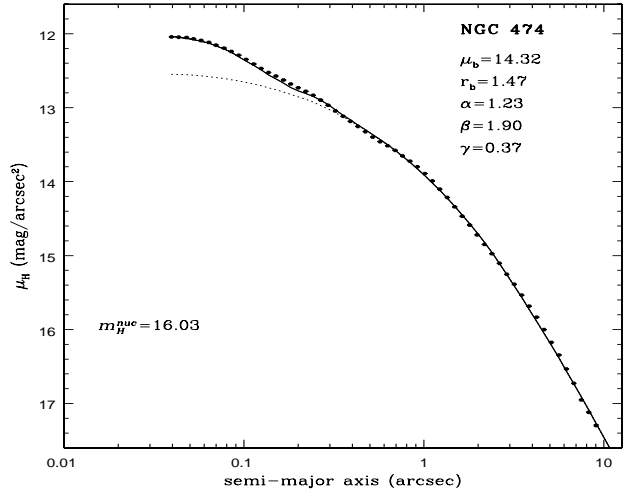
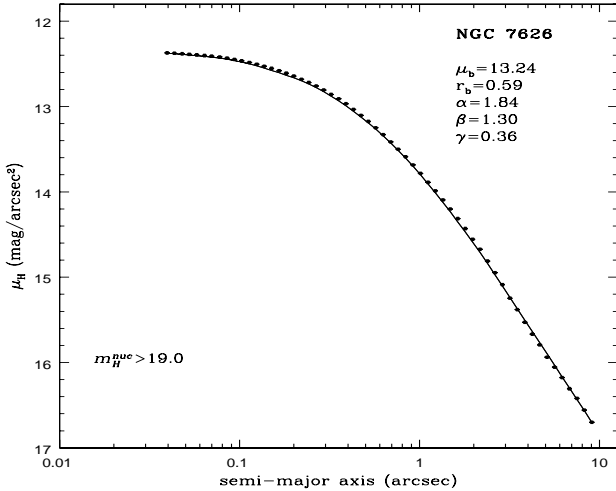
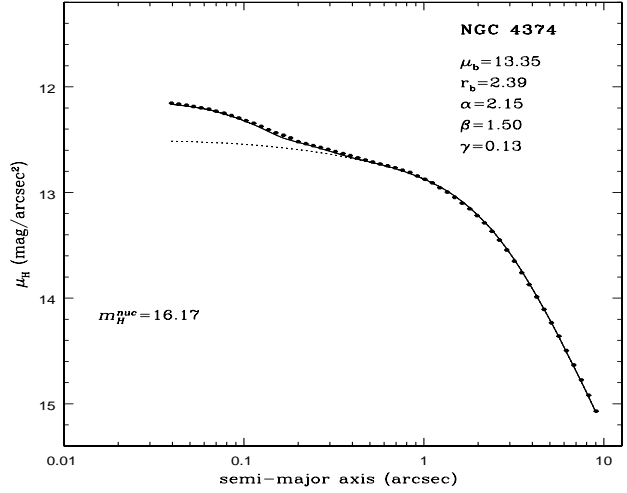
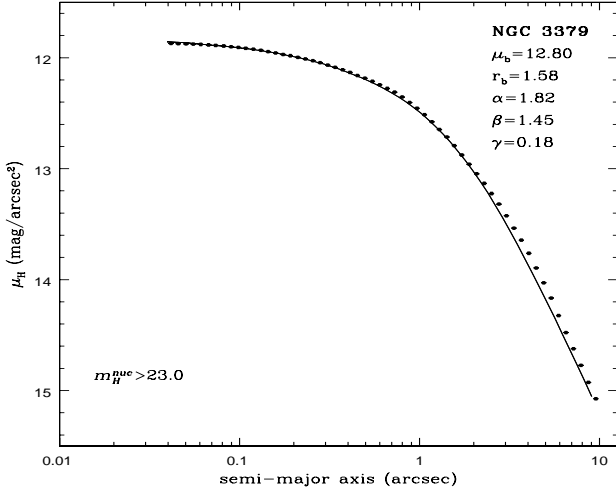


Fig. 2. Nuker-law fits to the core-type galaxy NGC 3379 (*top*) and the power-law galaxy NGC 7626 (*bottom*). The solid points represent the observed surface brightness profile. The solid line is the 1-D profile extracted from isophote fits to the generated model galaxy. Upper limits to nuclear magnitudes are given.

Fig. 3. Nuker-law fits with point source for the core-type galaxy NGC 4374 (*top*) and the power-law galaxy NGC 474 (*bottom*). The solid points represent the observed surface brightness profile. The solid line is the 1-D profile extracted from isophote fits to the generated model galaxy. The dotted line is the intrinsic bulge profile obtained by omitting the point source in the model.

lating over the bad pixels (Dickinson 1999). The ramp fitting procedure used in the CalnicA removes most of the cosmic rays from the images. Residual cosmic rays, defective pixels, and the coronagraphic hole (in NIC2 images) were masked during further analysis.

3. Isophotal Analysis

The *ellipse* task available in STSDAS was used to fit elliptical isophotes to the galaxy images and thereby obtain the surface brightness profiles and the radial variation of ellipticity and position angle. The results of the isophotal analysis were used to create smooth model images of the galaxies, and residual images which highlight the high-spatial frequency features were obtained by subtracting

the model images from the observed images. The presence of features such as dust and weak disks causes variations in ellipticity and P.A. The deviation from perfect elliptical isophotes can be expressed as a Fourier series, and the Fourier coefficient of the fourth cosine term in the expansion series (B4) is negative for boxy isophotes and positive for disk-like isophotes (Jedrzejewski 1987). The results from the isophotal analysis are shown in Figure 1 for NGC 4374, in which dust is revealed in the residual image, and for NGC 3115, which has a dominant stellar disk. Notice that the isophotes tend to get boxy around $r = 0''.2 - 0''.8$ in the case of NGC 4374 due to the dust lanes.

4. 2-D Modeling Using Analytic Functions

Earlier *HST* studies of the central surface brightness profiles of galaxies involved deriving the central parameters by fitting the 1-D profiles with analytic functions. The uncertainties caused by the PSF were overcome by performing the fits on profiles derived from deconvolved images (Lauer et al. 1995) or by convolving the analytic 1-D fits with the PSF and then comparing to the observed profiles (Carollo & Stiavelli 1998). Most of the data used in the present work were obtained through snapshot survey programs and do not have the high S/N required to perform reliable deconvolution of the images. Since a more reliable approach would be to sample the PSF in two dimensions, we choose to parameterize the galaxy bulge through a 2-D modeling using analytic functions and convolving the model image with the 2-D PSF image. This was done using the GALFIT program (Peng et al., in preparation), which enables us to create model images for different analytic functions (e.g., Sérsic/de Vaucouleurs, Nuker, exponential, Gaussian) and convolve them with the PSF. In lieu of observing PSFs simultaneously, TINYTIM simulations provide a good alternative (Krist & Hook 1997). GALFIT allows modeling the contribution from unresolved point sources or resolved star clusters in addition to the underlying galaxy. The program outputs the fit parameters for the galaxy and the point source or star cluster, along with images of the model galaxy and residuals. Following the results from earlier *HST* studies of early-type galaxies, we modeled the galaxy light using the empirical Nuker function. When appropriate, we also fit a compact source simultaneously in order to deblend a component in excess of the underlying galaxy component. When no compact source was required, we obtained an upper limit to the point source magnitude. A comparison of the 1-D surface brightness profiles derived by doing ellipse-fits on the observed image and the model image created by GALFIT, shows that the 2-D modeling reproduces the observed profiles very well (Figures 2 and 3).

5. Results

5.1. Properties of the Host Galaxies

Early-type galaxies appear to have a smooth light distribution in the *H* band, showing dust features only in very few cases, mostly associated with galaxies hosting unresolved nuclei (e.g., NGC 1052, 4150, and 4374). The presence of dust in some cases is found to cause boxiness of the isophotes resulting in negative B4 values. We confirm the results from earlier studies that core galaxies are luminous elliptical galaxies with boxy or neutral isophotes, while power-law galaxies have low luminosities and disk isophotes (Faber et al. 1997). However, we do not find a dichotomy in the inner slope values (Ravindranath et al. 2001). Instead, we find a continuous distribution of γ values similar to that found by Carollo et al (1997)

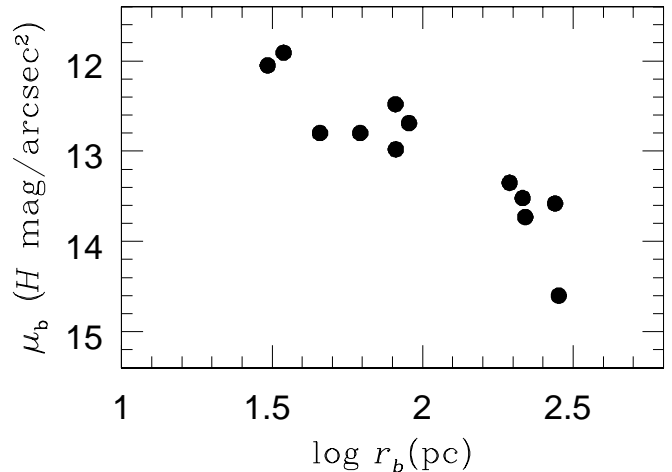


Fig. 4. The FP relation between μ_b and r_b for core galaxies.

for their sample of ellipticals with kinematically distinct cores. Core galaxies obey the fundamental-plane (FP) relations in the $(\log r_b, \mu_b)$ -plane with brighter galaxies having larger cores with lower surface brightness (Figure 4).

5.2. Properties of Unresolved Nuclei

About one-third of our sample galaxies have clear evidence for the presence of an unresolved central compact source, and the frequency of occurrence of point sources is almost equal for core galaxies and power-law galaxies. However, all the central sources associated with core galaxies are AGNs by their nuclear spectral classification, while power-law galaxies mostly contain absorption-line nuclei, transition objects, and weak AGNs. Most type 1 Seyfert and LINER nuclei (5 out of 6) have point sources compared to type 2 nuclei (5 out of 14). The unresolved nuclei have magnitudes in the range $13.5 \leq m_H \leq 17.3$, with the exceptionally bright Seyfert nucleus in NGC 5548 having $m_H = 11.9$ mag.

References

- Carollo, C.M., Franx, M., Illingworth, G.D., & Forbes, D.A., 1997, *ApJ* 481, 710
 Carollo, C.M., & Stiavelli, M., 1998, *AJ* 115, 2306
 Dickinson, M., 1999, *NICMOS Instrument Handbook*, version 4.0 (Baltimore: STScI)
 Faber, S.M., et al., 1997, *AJ* 114, 1771
 Ferrarese, L., et al., 1994, *AJ* 108, 1598
 Ho, L.C., Filippenko, A.V., & Sargent, W.L.W., 1997, *ApJS* 112, 391
 Jedrzejewski, R.I., 1987, *MNRAS*, 226, 747
 Krist, J.E., & Hook, R.N., 1997, *1997 HST Calibration Workshop*, STScI, eds. S. Casertano et al.
 Lauer, T.R., et al., 1995, *AJ* 110, 262
 Ravindranath, S., et al., 2001, *in preparation*
 Quillen, A.C., Bower, G.A., & Stritzinger, M., 2000, *ApJS* 128, 85